Eur Biophys J (2011) 40:599–610
DOI 10.1007/s00249-010-0654-3

ORIGINAL PAPER

Biophysical characterization of *Entamoeba histolytica* phosphoserine aminotransferase (EhPSAT): role of cofactor and domains in stability and subunit assembly

Vibhor Mishra · Vahab Ali · Tomoyoshi Nozaki · Vinod Bhakuni

Received: 3 October 2010 / Revised: 21 November 2010 / Accepted: 25 November 2010 / Published online: 16 December 2010

Abstract We investigated the role of the cofactor PLP and its binding domain in stability and subunit assembly of phosphoserine aminotransferase (EhPSAT) from an enteric human parasite *Entamoeba histolytica*. Presence of cofactor influences the tertiary structure of EhPSAT because of the significant differences in the tryptophan microenvironment and proteolytic pattern of holo- and apo-enzyme. However, the cofactor does not influence the secondary structure of the enzyme. Stability of the protein is significantly affected by the cofactor as holo-enzyme shows higher T_m and C_m values for thermal and GdnHCl-induced denaturation, respectively, when compared to the apo-enzyme. The cofactor also influences the unfolding pathway of the enzyme. Although urea-dependent unfolding of both holo- and apo-EhPSAT is a three-state process, the intermediates stabilized during unfolding are significantly different. For holo-EhPSAT a dimeric holo-intermediate was stabilized, whereas for apo-EhPSAT, a monomeric intermediate was stabilized. This is the first report on stabilization of a holo-dimeric intermediate for any aminotransferase. The isolated PLP-binding domain is stabilized as a monomer, thus suggesting that either the N-terminal tail or the C-terminal domain of EhPSAT is required for stabilization of dimeric configuration of the wild-type enzyme. To the best of our knowledge, this is a first report investigating the role of PLP and various protein domains in structural and functional organization of a member of subgroup IV of the aminotransferases.

Keywords EhPSAT · *Entamoeba histolytica* · Phosphoserine aminotransferase · Pyridoxal-5′-phosphate · Denaturation · PLP-binding domain

Abbreviations

PSAT	Phosphoserine aminotransferase
PLP	Pyridoxal-5′-phosphate
Ni-NTA	Nickel nitrilotriacetic acid
SEC	Size exclusion chromatography

Introduction

More than 30 percent of the known proteins require cofactors for their ideal biological function (Deu and Kirsch 2007a). In some cases the cofactor guides the folding pathway of protein by binding to the partially unfolded state or associating with the native conformation of the protein (Bollen et al. 2005; Muralidhara and Wittung-Stafshede 2005). For large multi-domain and oligomeric proteins, the cofactor stabilizes its binding domain (Wardell et al. 2005) or the quaternary structure if present at the subunit interface (Pant and Crane 2005). However, for certain proteins the cofactor interacts with the

Electronic supplementary material The online version of this article (doi:10.1007/s00249-010-0654-3) contains supplementary material, which is available to authorized users.

V. Mishra · V. Bhakuni (✉)
Division of Molecular and Structural Biology, Central Drug Research Institute, Lucknow 226001, India
e-mail: bhakuniv@rediffmail.com

V. Ali
Department of Biochemistry, Rajendra Memorial Research Institute of Medical Sciences, Agam Kuan, Patna 800007, India

T. Nozaki
Department of Parasitology, National Institute of Infectious Diseases, 1-23-1 Toyama, Shinjuku-Ku, Tokyo 162-8640, Japan

protein in the later stages of folding and has no contribution in its folding mechanism (Cai et al. 1995). Pyridoxal-5′-phosphate (PLP) represents one of the most versatile cofactors (Schneider et al. 2000) as there is a wide variety of structural diversity among the PLP-dependent enzymes (Jansonius 1998; Schneider et al. 2000). Aminotransferases (AT) (EC2.6.2.X) belong to the large α family of PLP-dependent enzymes. ATs are subdivided into four subclasses (Mehta et al. 1993), namely subclass I, II, III and IV. The members of I, II and IV subclasses belong to fold type I, while subclass III belongs to fold type IV. In all the ATs the cofactor is positioned at the active site and serves as an epicenter for structural and functional features of the protein. Removal of the cofactor from these proteins leads to loss of their activity and induces considerable changes in their structure (Schneider et al. 2000). The isolated PLP-binding domain behaves as an autonomous folding/unfolding unit both under in vitro as well as in vivo conditions (Herold et al. 1991).

EhPSAT is a member of subclass IV of the ATs (Hester et al. 1999). It is a homodimer of ~86 kDa molecular mass having two molecules of PLP per molecule of the enzyme (Ali and Nozaki 2006; Mishra et al. 2010). Based on the in silico modeling of EhPSAT using *Escherichia coli* PSAT and *Bacillus alkalophilus* PSAT crystal structures as template, it was observed that each subunit of the enzyme is comprised of two domains (Fig. 1a), a large PLP-binding domain (residue 16–268) (Fig. 1b, c), a N-terminal tail (residue 1–15) and a C-terminal domain (residue 269–358) (Fig. 1d). As the active site is nested at the subunit interface, a complete dimer is essentially required for enzymatic activity (Ali and Nozaki 2006; Mishra et al. 2010). The majority of the inter-subunit interactions are constituted by the interface residues of the two large PLP-binding domains. The unusual structural features of PSAT make its structure the smallest among all of its family proteins (Hester et al. 1999).

To understand the role of the cofactor on structural and stability features of the protein as well as the role of various structural domains towards stabilization of native conformation of the enzyme, we performed an extensive comparative analysis of structural, stability and unfolding characteristics of holo and apo forms of purified recombinant EhPSAT and its PLP-binding domain (PLPbd).

Materials and methods

Materials

All chemicals used in the study were purchased from Sigma-Aldrich Chemical Company, St Louis, MO. The SEC columns were purchased from GE Health Care. MilliQ (Millipore) water was used for all the buffer preparations and bacterial cell culture.

Methods

Overexpression and purification of EhPSAT

The overexpression and purification of recombinant EhPSAT were carried out as described earlier (Mishra et al.

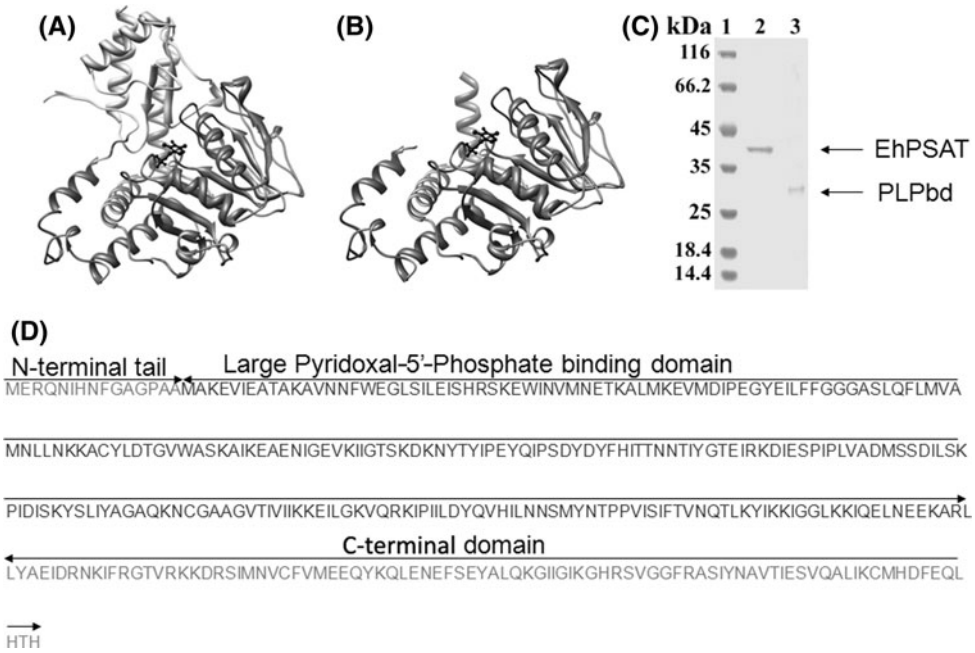

Fig. 1 Analysis of various domains of EhPSAT. **a** and **b** Homology model of an EhPSAT subunit. The PLP-binding domain is shown in dark grey, and the C-terminal domain in *light grey* colors. The cofactor PLP is shown in *black* color. **c** SDS-PAGE analysis. *Lanes 1–3* represent molecular weight markers, EhPSAT and PLPbd. **d** Amino acid sequence analysis of the EhPSAT. The N-terminal tail (residue 1–15), the PLP-binding domain (residue 16–268) and the C-terminal domain (residue 269–358)

2010). Apo-enzyme was prepared as described earlier (Deu and Kirsch 2007b) and confirmed by measuring the loss of activity and near-UV CD signal.

Cloning, overexpression and purification of the pyridoxal-5′-phosphate binding domain (PLPbd) of EhPSAT

The PLP-binding domain (PLPbd) (Met^{16}–Leu^{268}) of EhPSAT encoded by a 759 base pair (bp) gene fragment was PCR amplified from the full length gene of EhPSAT (pTZ57R/T-EhPSAT). The PCR was performed with primers (forward-5′-GCTAGCATGGCGAAAGAAGTTA TTGAGGCGACGGCA-3′ and reverse-5′-AAGCTTCAAT CGAGCCTTTTCTTCATTTAATTCTTGTAT-3′) with NheI and HindIII restriction sites. PCR conditions used were: 1 × 94°C for 5 min, 30 × 94°C for 45 s, 50°C for 45 s and 72°C for 2 min and finally 1 × 72°C for 10 min. The amplified DNA fragment was cloned in pTZ57R/T (InsTAclone™ PCR cloning kit, Fermentas) cloning vector. The resultant construct was subsequently double digested with the respective restriction enzymes, and the DNA fragment (759 bp) obtained was further sub-cloned into pET23a (+) vector (Novagen) between NheI and HindIII sites. The resultant constructs were transformed into *E.coli* C41 competent cells for expression. A single colony of C41 LB ampicillin plate was inoculated into 5 ml of LB broth (HI media) having ampicillin at a concentration of 100 μg/ml and allowed to grow overnight at 37°C. It was then subcultured in a 500-ml LB broth at 37°C until A_{600} of 0.6 was achieved. The culture was then induced with 1 mM of isopropyl-1-thio-*β*-D-galactopyranoside and was further incubated at 20°C for 16 h. The cells were harvested at 8,000 rpm for 10 min, and the resultant pellet was resuspended in 50 mM potassium phosphate (pH 8) buffer containing 300 mM NaCl, 2 mM PMSF, 5 mM imidazole, 2 mM EDTA, 2 mM DTT and 10% glycerol. Cells were disrupted using a probe type sonicator and centrifuged at 13,500 rpm for 30 min. The supernatant was applied on nickel nitrilotriacetic acid (NiNTA) agarose affinity column pre-equilibrated with 50 mM potassium phosphate (pH 8) buffer along with 300 mM NaCl and 5 mM imidazole. The column was subsequently washed with two column volumes of the same buffer containing 5 mM and one column volume each of 20 mM and 40 mM imidazole, respectively. The protein was eluted using 500 mM imidazole. The eluted protein was tested for purity by SDS-PAGE and ESI-MS and was >95% pure.

GdnHCl and urea denaturation

In the presence and absence of increasing concentrations of GdnHCl/urea, 3 μM protein (EhPSAT or PLPbd) was dissolved in potassium phosphate buffer (50 mM, pH 8.0) and was then incubated overnight at 25°C before measurements were made. Overnight incubation time was sufficient for the reaction to achieve equilibrium under all denaturant concentrations.

Spectrophotometric measurements

Fluorescence spectra were recorded on a Perkin Elmer LS50b luminescence spectrometer at 25°C. For tryptophan fluorescence an excitation wavelength of 280 nm and emission wavelength of 300 nm and 400 nm were used. For ANS binding studies, a dye:protein ratio of 5:1 was used. Samples were incubated with ANS for 1 h with gentle shaking before taking measurements. For fluorescence measurement excitation wavelength was 365 nm, and emission was monitored between 400 nm and 600 nm. Fluorescence polarization for the reduced cofactor was measured at a fixed wavelength of 386 nm, and the excitation wavelength was fixed at 335 nm.

CD experiments were performed with a JASCO J810 spectropolarimeter (equipped with peltier temperature controller system) in a 0.2-cm cell at 25°C. The CD spectra were measured at an enzyme concentration of 3 and 15 μM for far-UV and near-UV CD measurements. Readings obtained were normalized by subtracting the baseline observed for the buffer with similar denaturant concentration under similar conditions. Thermal denaturation was carried out by monitoring changes in the CD ellipticity at 222 nm at a constant rate of 1°C/min.

The residual activity of the overnight denaturant incubated protein samples was assessed by diluting an aliquot of the sample into assay buffer [50 mM potassium phosphate buffer, 0.1 mM NADH, 32 mM ammonium acetate, 2.0 mM glutamate, 0.35 mM phosphohydroxy pyruvate (PHP), 1 U gulamate dehydrogenase (GDH) at pH 8.0] and measuring the initial activity with the GDH coupled assay. The decrease in NADH concentration was monitored at 340 nm on a Shimadzu UV 1650PC spectrophotometer at 25°C (Ali and Nozaki 2006). PLP was omitted from the reaction mixture to avoid reconstitution of the holoenzyme. No increase in the activity was observed during the time of the assay. Control experiments show that the residual denaturant has no effect on the rates of the GDH-coupled reactions.

Glutaraldehyde crosslinking

The crosslinking of protein samples equilibrated overnight at the desired denaturant concentration was carried out as described earlier (Mishra et al. 2010) and analyzed on 10% SDS-PAGE.

Size exclusion chromatography (SEC)

Gel filtration experiments were carried out on a Superdex^{TM} 200, 10/300GL and Superdex^{TM} 75, 10/300GL column on AKTA FPLC (GE Health care) pre-calibrated with standard molecular weight markers. The columns were pre-equilibrated and run with 50 mM potassium phosphate buffer, pH 8, with or without the desired denaturant concentration at 25°C at a flow rate of 0.3 ml/min with detection at 280 and 415 nm.

Limited proteolysis

The protein was subjected to limited proteolysis with α-chymotrypsin at a protease to protein ratio of 1:300 for 20 min at 25°C. The protease reaction was stopped by addition of phenyl-methyl-sulfonyl fluoride (PMSF) to a final concentration of 1 mM in the reaction mixture, and the samples were analyzed on 12% SDS-PAGE.

Homology modeling and amino acid sequence analysis

The homology model of the EhPSAT subunit was generated using a Swiss Model Server (Schwede et al. 2003) with Protein Data Bank (PDB) I.D. 1W23 taken as a template, and the image obtained was visualized using the UCSF Chimera (Pettersen et al. 2004). The amino acid sequence of EhPSAT (systematic I.D. 30.m00263) was extracted from the geneDB *Entamoeba histolytica* database. The protein-protein interaction analysis of EhPSAT homodimer was performed using CONPLEX web-based server (Choi et al. 2010).

Results

Effect of cofactor PLP on structural and stability features of EhPSAT For PSAT the cofactor PLP serves as an epicenter for proper conformation as well as stabilization of the active site (Hester et al. 1999; Kapetaniou et al. 2006). Comparative studies on holo- and apo-EhPSAT using optical spectroscopic techniques were performed to understand cofactor-induced changes in protein structure and stability. EhPSAT showed a characteristic positive near-UV CD signal at 410–415 nm, which subsequently got lost on removal of cofactor (Fig. 2a).

Secondary structure Far-UV CD spectra of holo- and apo-EhPSAT show presence of a typical α/β type secondary structure. The content of the secondary structure was analyzed using K2D software (Andrade et al. 1993). The percentage of secondary structure elements was similar in both forms of the enzyme, thereby suggesting that the removal of cofactor does not lead to any significant alterations in the secondary structure of the enzyme (Fig. 2b).

Tertiary structure The tryptophan emission wavelength maximum for holo-EhPSAT was observed at 333 nm (Fig. 2c). Buried tryptophan residues in a folded protein show fluorescence emission maxima between 330 and 335 nm (Lakowicz 2006). For apo-EhPSAT, a shift in tryptophan emission wavelength maxima to 340 nm was observed (Fig. 2c). This suggests a partial exposure of the buried hydrophobic interiors of the protein on removal of the cofactor PLP. This suggestion was further supported by the binding of ANS to the apo-enzyme as observed by a shift in wavelength maxima and enhancement in fluorescence intensity of ANS in the presence of apo-enzyme only (Fig. 2d).

Comparative changes in the tertiary structure of holo- and apo-EhPSAT were also analyzed by limited proteolysis using α-chymotrypsin. The apo-EhPSAT showed significant fragmentation, whereas the holo-enzyme was resistant to the proteolysis under similar conditions (Fig. 2d inset). These observations collectively demonstrate that the tertiary structure of EhPSAT is significantly perturbed on removal of the cofactor PLP from the enzyme.

Cofactor PLP imparts stability to EhPSAT Comparative thermal stability of holo- and apo-EhPSAT was studied by monitoring changes in the CD signal at 222 nm as a function of temperature. For both forms of the enzyme a cooperative thermal denaturation of the protein was observed. However, for the holo-enzyme a T_m of about 67°C was observed that was significantly higher than the T_m of about 55°C observed for the apo-enzyme (Fig. 2e). This demonstrates that loss of cofactor PLP leads to a decrease in the stability of EhPSAT.

GdnHCl-induced denaturation Equilibrium unfolding studies of a protein using denaturants provide a measure of its conformational stability (Greene and Pace 1974; Knapp and Pace 1974; West and Price 1989). The GdnHCl-induced alterations in the tertiary and secondary structure of holo- and apo-EhPSAT were monitored by studying changes in the tryptophan fluorescence and far-UV CD signal at 222 nm, respectively, of the enzyme at increasing GdnHCl concentrations (Fig. 2f). The denaturation curves showed a superimposible sigmoidal dependence of these changes suggesting GdnHCl-induced unfolding of EhPSAT to be a two-state process. For proteins with two-state transition, the C_m value obtained from the analysis of the solvent denaturation curve intrinsically serves as a probe for its stability to the chaotrope (Akhtar et al. 2002; Deu and Kirsch 2007a). Interestingly the C_m values obtained from the denaturation profile for holo-EhPSAT and apo-EhPSAT were 2.8 and 2 M, respectively. The C_m observed for the apo-enzyme was considerably lower than for the

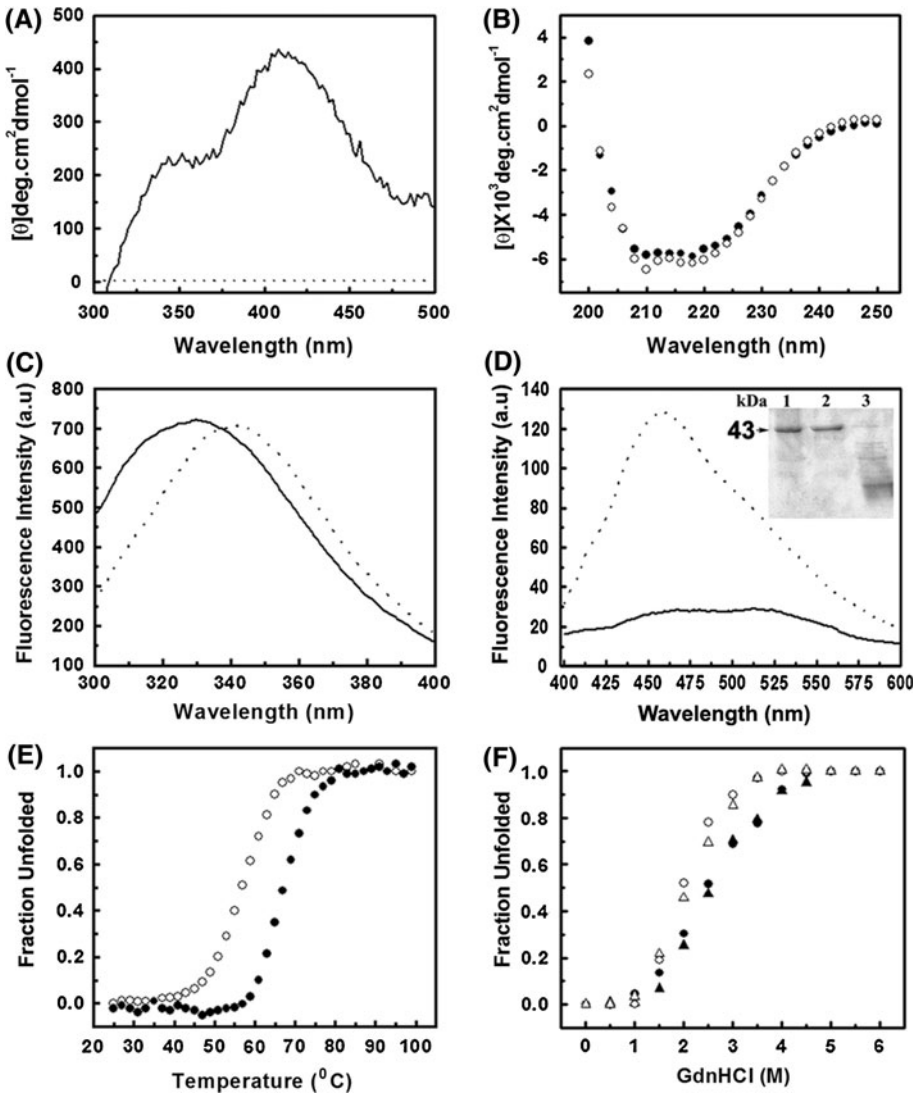

Fig. 2 Effect of cofactor PLP on structural and stability features of EhPSAT. **a** Near-UV CD spectra of holo- (*solid line*) and apo- (*dashed line*) EhPSAT. **b** Far-UV CD spectra of holo- (*filled circle*) and apo- (*open circle*) EhPSAT. **c** Fluorescence emission spectra of holo- (*solid line*) and apo- (*dotted line*) EhPSAT. **d** ANS fluorescence spectra of holo- (*solid line*) and apo-EhPSAT (*dotted line*). *Inset* shows SDS-PAGE profile obtained from limited proteolysis of holo- and apo-EhPSAT with α-chymotrypsin. *Lanes 1–3* represent native protein, EhPSAT holo-enzyme and EhPSAT apo-enzyme, respectively. **e** Thermal unfolding profile of holo- (*filled circle*) and apo- (*open circle*) EhPSAT as monitored by loss of CD signal at 222 nm. A linear extrapolation of baselines in pre- and post-transition regions was used to determine the fraction of unfolded protein within the transition region by assuming a two-state mechanism of unfolding. The thermal transition of the enzyme was irreversible with precipitation observed at the end of the scan. **f** GdnHCl-induced denaturation of EhPSAT as monitored by changes in tryptophan fluorescence emission maxima for holo-enzyme (*filled triangle*), apo-enzyme (*open triangle*) and loss of CD ellipticity at 222 nm for holo-enzyme (*filled circle*) and apo-enzyme (*open circle*), respectively. All samples were incubated overnight at different denaturant concentrations

holo-enzyme, suggesting that loss of the cofactor leads to destabilization of the protein.

Unfolding of holo- and apo-EhPSAT in urea

EhPSAT holo-enzyme

Tryptophan fluorescence has been used extensively to obtain information on the structural and dynamic properties of the protein (Akhtar et al. 2002). Figure 3a illustrates changes in the tryptophan emission wavelength of the EhPSAT holo-enzyme with respect to increasing urea concentrations. An initial sigmoidal increase in the tryptophan emission maxima from 335 to 340 nm was observed between 0 and 3 M urea. Between 3 and 4 M urea, no significant change in emission wavelength maxima was observed, indicating stabilization of an intermediate state. With a further increase in the urea concentration

between 4 and 8.5 M, a second transition was observed with an increase in tryptophan emission maxima from 340 to 355 nm.

The above-mentioned changes in the tertiary structure for the holo-enzyme prompted us to investigate changes in the enzymatic activity as a function of denaturant concentration. Activity of the enzyme is considered the most sensitive probe to study the changes in an enzyme's conformation as it reflects subtle readjustments at the active site, allowing very small conformational variations in structure to be detected (Singh and Bhakuni 2008). Figure 3b summarizes the effect of increasing concentrations of urea on the enzymatic activity of EhPSAT. A steep decrease of enzymatic activity from 100% to almost 0% was observed between 0 and 4 M urea. Spectral characteristics of the PLP could invariably serve as a marker for observing conformational changes in the active site microenvironment (Cai et al. 1995; Mishra et al. 2010). The effect of urea on the PLP microenvironment as studied by monitoring changes in fluorescence polarization with increasing urea concentration is summarized in Fig. 3b. A sharp decrease in polarization values between 0 and 4 M urea was observed, demonstrating a significant alteration in the PLP microenvironment under these conditions. Together these observations suggest that loss of enzymatic activity with increasing urea concentration occurs because of urea-induced changes in the PLP microenvironment.

Figure 3a summarizes the effect of increasing urea concentration on the CD ellipticity at 222 nm for holo-EhPSAT. Initially, up to 2.5 M urea, no change in the CD ellipticity was observed; however, between 2.5 and 3 M urea a sharp loss of about 30% in secondary structure was observed, which remained constant up to 4 M urea. Interestingly, between 0 and 2.5 M urea, no significant change in the secondary structure of the enzyme was observed; however, under similar conditions a significant change in tertiary structure was observed (discussed earlier). These observations suggest that urea-induced changes in the secondary structure occur only after significant perturbations in the tertiary structure of the enzyme.

SEC experiments were performed to analyze changes in the quaternary structure of the enzyme in the presence of increasing urea concentration as shown in Fig. 3c. The SEC profile of EhPSAT incubated and run in the presence of buffer containing 4 M urea showed a decrease in the retention volume (13.7 ml) as compared to the native enzyme (14.3 ml). The superimposition of absorbance at 415 nm (corresponding to PLP) and 280 nm (corresponding

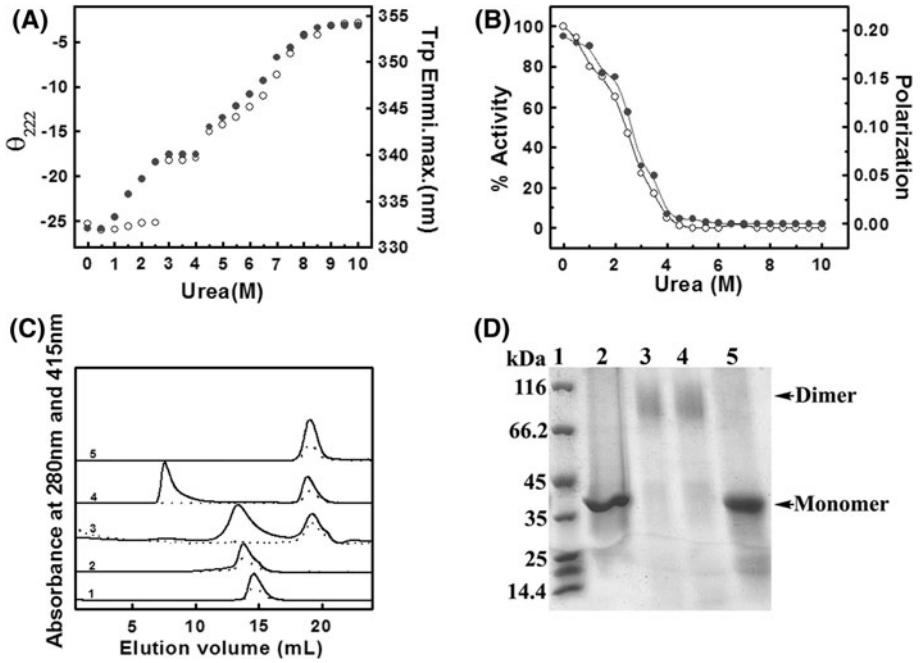

Fig. 3 Urea-induced unfolding of holo-EhPSAT. **a** Urea-induced denaturation of holo-EhPSAT as monitored by changes in tryptophan fluorescence emission maxima (*filled circle*) and CD ellipticity at 222 nm (*open circle*). All samples were incubated overnight at different denaturant concentrations. **b** Changes in enzymatic activity of EhPSAT on incubation with increasing concentrations of urea (*open circle*). Data are plotted as percentages with enzymatic activity observed for EhPSAT in the absence of urea taken as 100%. The changes in the cofactor fluorescence polarization with increasing concentrations of urea are shown with (*filled circle*). **c** SEC profiles of EhPSAT on a Superdex^{TM} 200 10/300GL column. Profiles 1–5 represent enzyme samples of 0, 4, 5 and 8.5 M urea-treated holo-EhPSAT and PLP alone, respectively. *Solid and dotted lines* represent absorbance at 280 and 415 nm, respectively. **d** The 10% SDS-PAGE profile of glutaraldehyde crosslinked urea-treated samples of holo-EhPSAT. *Lanes 1–5* represent molecular weight markers, uncrosslinked native protein and crosslinked samples of 0, 4 and 8.5 M urea-treated samples, respectively

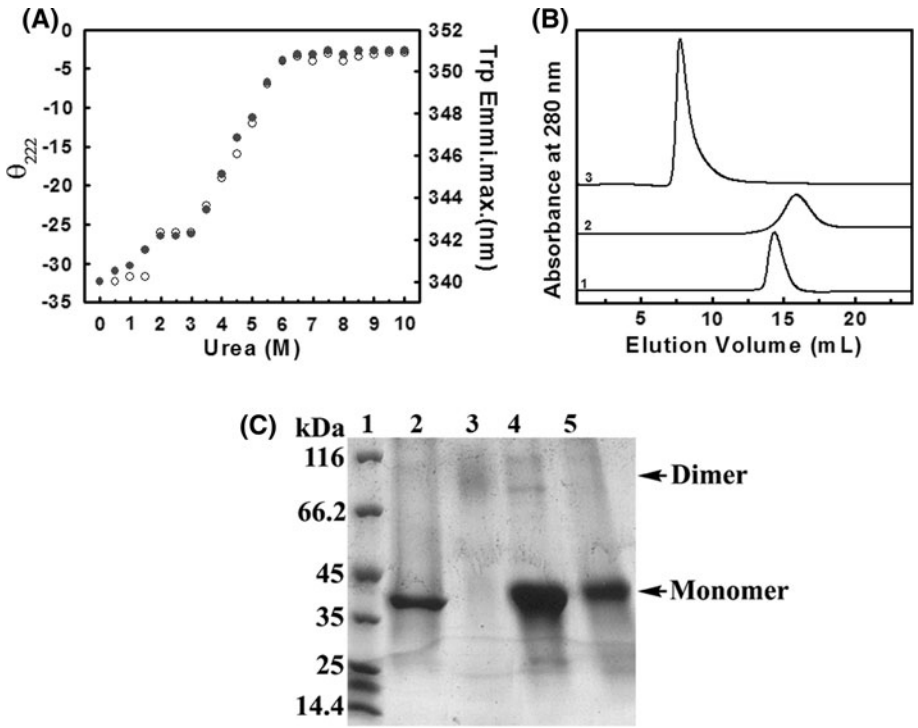

Fig. 4 Urea-induced unfolding of apo-EhPSAT. **a** Urea-induced denaturation of apo-EhPSAT as monitored by tryptophan fluorescence (*filled circle*) and CD ellipticity at 222 nm (*open circle*). All samples were incubated overnight at different denaturant concentrations. **b** SEC profiles on Superdex^{TM} 200 10/300GL column; profiles 1–3 represent samples of 0, 3 and 8.5 M urea-treated apo-EhPSAT, respectively. **c** The 10% SDS-PAGE profile of glutaraldehyde crosslinked urea-treated samples of apo-EhPSAT. *Lanes 1–5* represent molecular weight marker uncrosslinked native protein and crosslinked samples of 0, 3 and 8.5 M urea-treated samples, respectively

to aromatic amino acids) under these conditions suggests that the cofactor was still attached to the intermediate state stabilized under these conditions. A further increase in the urea concentration to 5 M resulted in reduction of the retention volume to 13.5 ml with release of the cofactor, as observed from a separate peak at 20 ml (corresponding to free PLP) under these conditions. At 8.5 M urea, the protein eluted in void volume (8.2 ml), which was due to complete unfolding of the enzyme resulting in significant enhancement in the hydrodynamic radii of the enzyme. The effect of urea denaturation on the subunit configuration was further studied by a glutaraldehyde-mediated crosslinking experiment. For native 4 M urea and 5 M (data not shown) urea-incubated samples, single protein bands corresponding to the enzyme dimer were observed. For 8.5 M urea denatured protein, a single band corresponding to the enzyme monomer was observed, which along with the SEC results (discussed above) confirms the presence of unfolded monomer under these conditions (Fig. 3d).

The results of urea-induced unfolding of the holo-EhPSAT demonstrate that low urea concentration leads to the accumulation of a dimeric holo-intermediate that subsequently undergoes simultaneous dissociation and unfolding at higher urea concentration.

PSAT apo-enzyme

For the apo-EhPSAT, changes in the secondary and tertiary structure as a function of denaturant concentration were monitored by tryptophan fluorescence and far-UV CD studies, respectively. The results demonstrate stabilization of a partially folded intermediate at low urea concentration (2–3 M), followed by complete unfolding of protein at higher denaturant concentration (Fig. 4a).

Figure 4b summarizes changes in the molecular dimension of the apo-EhPSAT at 0, 3 and 8.5 M urea as monitored by SEC. The apo-EhPSAT is stabilized as a dimer; however, at 3 M urea a significant enhancement in the retention volume (15.8 ml) for the protein was observed, suggesting a significant decrease in the hydrodynamic radii of the protein. Such a change in the hydrodynamic radii of a protein can happen only under two conditions: (1) if urea induces compaction in dimeric configuration of enzyme or (2) if the dimeric apo-EhPSAT dissociates into monomer in the presence of urea.

Presence of a single protein band of 43 kDa molecular mass for 3 M urea-treated protein in glutaraldehyde crosslinking experiments demonstrates that the dissociation of dimer into monomer occurs under these conditions (Fig. 4c).

Kirsch et al. identified two structural regions with distinct stabilities for *E. coli* AAT, the active site region (ASR) and the generally more stable dimerization region (DMR) (Deu and Kirsch 2007a). The DMR holds key intersubunit contacts, and its disorder leads to dimer dissociation (Deu and Kirsch 2007a). The observed early dissociation of dimeric apo-EhPSAT to monomer in the presence of low urea concentration indicates a possible influence of cofactor in the stabilization of the dimeric configuration of the enzyme in addition to its pivotal role in

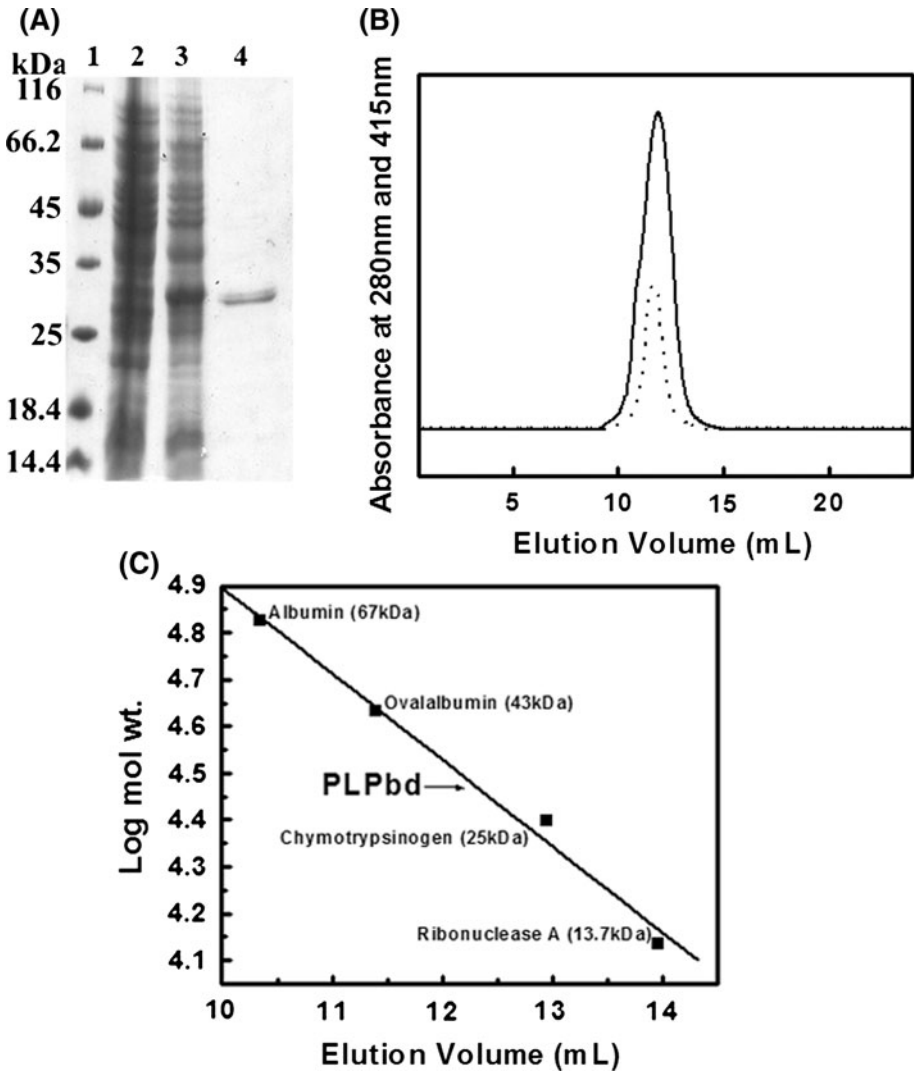

Fig. 5 Overexpression, purification and SEC profile of the PLP-binding domain (PLPbd). **a** SDS-PAGE analysis of *E. coli* C41 cell lysate overexpressing PLPbd and the purified protein. *Lanes 1–4* represent molecular weight markers, uninduced cell lysate, induced cell lysate and purified PLPbd. **b** SEC profile of PLPbd with absorbance at 280 nm (*solid line*) and absorbance at 415 nm (*dashed line*) on a Superdex^{TM} 75 10/300 GL column. **c** A graph for the log of molecular weight for standard protein markers (GE Health Care) plotted against their elution volume

the enzymatic activity. The loss of secondary and tertiary structure in the biphasic transition curve of the holo-EhPSAT suggests the possibility that the C-terminal domain might unfold prior to the denaturation of the larger PLP-binding domain. We further investigated the role of these domains separately in subunit assembly of the EhPSAT.

Characterization of the pyridoxal-5′-phosphate binding domain (PLPbd) of EhPSAT

The pyridoxal-5′-phosphate binding domain (PLPbd) of the EhPSAT was cloned, overexpressed and purified to homogeneity. The molecular mass of the recombinant PLPbd was about 28.38 kDa as observed on SDS-PAGE (Fig. 5a) and by ESI MS (data not shown). The molecular mass of PLPbd obtained by SEC was approximately 29 kDa (elution volume 11.98 ml), suggesting its stabilization as a monomer (Fig. 5b, c). This was further confirmed by chemical crosslinking, where a single protein band corresponding to a molecular mass of about 28 kDa was observed for the PLPbd on SDS-PAGE (data not shown). The near-UV CD spectrum of PLPbd showed the presence of cofactor PLP attached with the isolated domain (Fig. 6a). The recombinant domain showed a typical α/β type secondary structure (Fig. 6b). Amino acid sequence analysis and homology modeling (Mishra et al. 2010) showed the presence of three tryptophan residues in the large PLP-binding domain of the EhPSAT. The observed tryptophan fluorescence emission maxima of 340 nm for PLPbd suggest the presence of partially solvent exposed tryptophan residues in the native conformation of the purified domain (Fig. 6c).

The purified PLPbd was functionally inactive as each active site pocket is present at the subunit interface

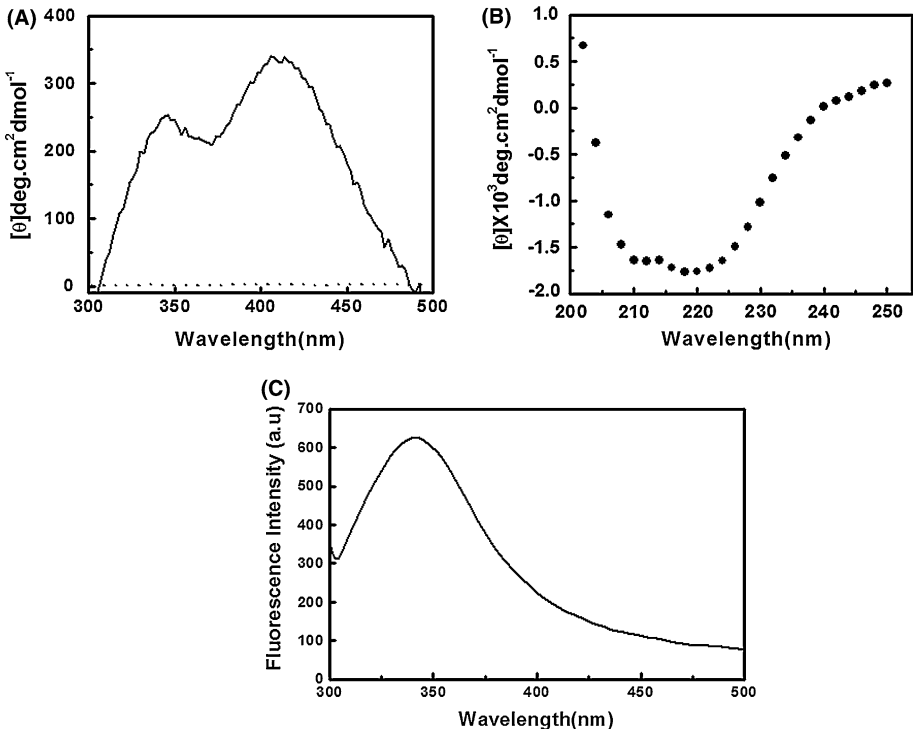

Fig. 6 Spectroscopic properties of the PLP-binding domain (PLPbd). **a** Near-UV CD spectra of the PLPbd. *Solid line* showing spectra for the holo domain and *dashed line* for the apo domain. **b** Far-UV CD spectrum of PLPbd (3 μM). **c** Tryptophan fluorescence emission spectrum of PLPbd. Excitation was at 280 nm and emission recorded from 300 to 500 nm

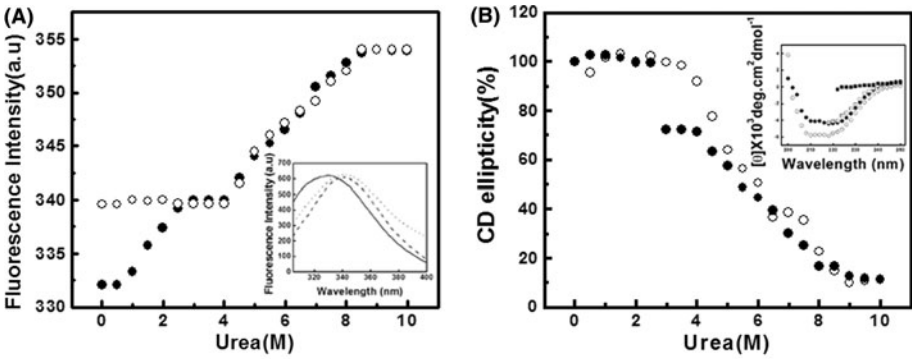

Fig. 7 Urea-induced equilibrium unfolding of PLPbd as monitored by changes in tryptophan fluorescence emission maxima and far-UV CD at 222 nm. **a** Urea-dependent unfolding of EhPSAT (*filled circle*) and PLPbd (*open circle*) monitored by changes in tryptophan fluorescence emission maxima. *Inset* showing the tryptophan fluorescence emission spectrum of EhPSAT holo-enzyme (*solid line*), EhPSAT incubated in 4 M urea (*dotted line*) and purified PLPbd (*dashed line*), respectively. **b** Urea-dependent unfolding of EhPSAT (*filled circle*) and PLPbd (*open circle*) monitored by CD ellipticity at 222 nm. The data are represented in percentage ellipticity at 222 nm taking the value for the native enzyme to be 100%. *Inset* showing far-UV CD spectra of EhPSAT holo-enzyme (*open circle*), PLPbd (*filled circle*), 4 M urea incubated EhPSAT (*open square*) and 8.5 M urea incubated EhPSAT (*filled square*), respectively

comprised of residues from both the PLP-binding domains of the two subunits and the C-terminal domain of the homodimer.

Equilibrium unfolding studies of PLPbd

Urea-induced unfolding of the PLPbd showed two-state transition, as monitored by the tryptophan fluorescence emission maxima and loss of CD ellipticity at 222 nm (Fig. 7a, b). Negligible changes in the tertiary as well as the secondary structure were observed up to 4 M urea; however, between 4 and 8 M urea a sigmoidal transition with complete denaturation at 8.5 M urea was observed. The C_m value for the domain was about 6 M, which was quite comparable to the C_m observed for the second transition of the biphasic curve during urea denaturation of the EhPSAT. The PLPbd showed tryptophan fluorescence emission maxima at 340 nm, which was also similar to the emission maxima observed for native holo-EhPSAT at 4 M urea (Fig. 7a inset). Furthermore, the far-UV CD spectrum of the intermediate stabilized at 4 M urea for holo-EhPSAT possesses about 70% signal of the native CD spectra. This

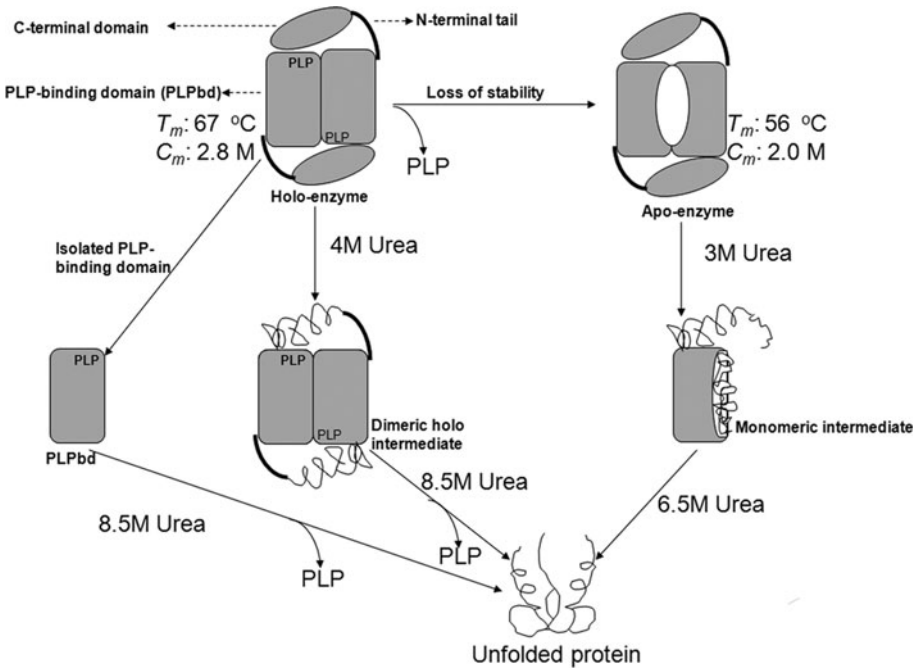

Fig. 8 Schematic diagram showing the effect of PLP and different domains on structural features of EhPSAT. The T_m and C_m values shown are observed by loss of secondary structure at 222 nm as a function of increasing temperature and loss of secondary and tertiary structure by GdnHCl-induced denaturation, respectively

is similar to the far-UV CD spectrum observed for PLPbd when an equimolar (considering the subunit structure) quantity of proteins was used for analysis (Fig. 7b inset). The unfolding studies of PLPbd demonstrate that it is an independent folding/unfolding domain of EhPSAT, which attains its structure before dimerization of the native protein molecule takes place. The self-illustrating model (Fig. 8) summarizes the structure and stability characteristics of holo- and apo-EhPSAT and a possible influence of the PLP-binding domain, N-terminal tail and C-terminal domain in stability and subunit assembly.

Discussion

EhPSAT belongs to subgroup IV of the aminotransferase family (Kapetaniou et al. 2006). It has significant structural differences with three other subgroups of the aminotransferases (Hester et al. 1999). The most remarkable difference is reduction of the structural N-terminal tail into a single β-strand (Hester et al. 1999). In addition, comparative analysis of EhPSAT with aspartate aminotransferase (AAT) (subgroup I), which is by far the most extensively studied aminotransferase, suggests significant differences in the relative orientation of their two domains (Hester et al. 1999).

GdnHCl-induced unfolding of holo- and apo-EhPSAT is a two-state process, whereas urea-induced unfolding of the enzyme is a three-state process. The exact molecular mechanism/s of the denaturation process induced by urea and GdnHCl have not yet been clearly defined (Makhatadze and Privalov 1992; Schellman 2002). It has been presumed that both urea and GdnHCl molecules unfold proteins by solubilizing the nonpolar parts of the protein molecule along with the peptide backbone CONH groups and the polar groups in the side chains of the protein (Nandi and Robinson 1984; Satterthwait and Jencks 1974). Accordingly the unfolding process of EhPSAT should follow the same path with both denaturants. However, significant differences in the unfolding pathway of EhPSAT were observed for urea and GdnHCl. This prompted us to look for other possible differences between the two denaturants, which would explain their different effects on the unfolding process.

GdnHCl is an electrolyte and therefore is expected to ionize into Gdn^+ and Cl^- ions in aqueous solution. From a structural point of view, urea and Gdn^+ are very similar; however, urea is a neutral (uncharged) molecule, whereas the guanidinium ion has a positive charge delocalized over the planar structure. At high concentrations, GdnHCl is a denaturant because the binding of Gdn^+ ions to the protein predominates and pushes the equilibrium towards the unfolded state. This results in denaturation of the protein. However, at low concentrations Gdn^+ ion can preferentially adsorb on the protein surface because of interactions with the negatively charged amino acid side chains present in the protein molecule. This would lead to perturbations and/or weakening of the optimized electrostatic interactions present in the native conformation of protein, and as a result more effective unfolding (unfolding at lower denaturant concentration) will be observed with GdnHCl as compared to urea.

Urea-induced denaturation studies of holo-EhPSAT and PLPbd suggest that the C-terminal domain unfolds prior to the PLP-binding domain. Studies also reflect the stabilization of an inactive dimeric holo-intermediate, which is otherwise very rare (Deu and Kirsch 2007b). The denaturation studies of holo-EhPSAT show the presence of two clear unfolding transitions. The first transition is that of the C-terminal domain followed by the dissociation of PLP from the protein in the second transition. For apo-EhPSAT denaturation, the structure of the PLP-binding domain is significantly perturbed along with the exposure of the hydrophobic interiors of the protein. In case of urea-induced unfolding, the apo-enzyme is stabilized as a monomeric intermediate at 3 M urea, whereas in case of *E. coli* apo-AAT a dimeric intermediate is stabilized during denaturation (Deu and Kirsch 2007a, b). Stabilization of the monomeric intermediate of apo-EhPSAT clearly suggests that the cofactor plays a significant role in maintaining the oligomeric status of EhPSAT. Protein-protein interaction analysis of the EhPSAT (supplementary Figure) shows that the majority of the inter-subunit interactions are present along the PLP-binding domain. The loss of cofactor leads to significant perturbation of these interactions along the dimer interface. Recent site-directed mutagenesis studies along ten different interface contacts of *E. coli* AAT suggest the absence of "hot spot" regions that stabilize the native protein; rather there is uniform distribution of noncovalent interactions along the PLP-binding domain and the N-terminal tail (Deu et al. 2009). In the present study, the stabilization of holo- and apo-EhPSAT intermediates is different in terms of their oligomeric structure, which suggests that not only the interaction between the protein domains but also the cofactor plays a significant role in the dimer stability.

Considering the wide array of PLP-binding proteins and their complexity, it is very difficult to draw a conclusion about their biophysical properties; however, the current study significantly contributes to an understanding of them.

Acknowledgments V.M. is grateful to the Council of Scientific and Industrial Research, Government of India, for the award of a research fellowship. Finally, we are thankful to Dr. Sohail Akhtar, Dr. Prabodh Kapoor and P. Shah for useful suggestions and for generating structural figures. This is communication no. 7996 from CDRI, India.

References

Akhtar MS, Ahmad A, Bhakuni V (2002) Guanidinium chloride- and urea-induced unfolding of the dimeric enzyme glucose oxidase. Biochemistry 41:3819–3827

Ali V, Nozaki T (2006) Biochemical and functional characterization of phosphoserine aminotransferase from *Entamoeba histolytica*, which possesses both phosphorylated and non-phosphorylated serine metabolic pathways. Mol Biochem Parasitol 145:71–83

Andrade MA, Chacon P, Merelo JJ, Moran F (1993) Evaluation of secondary structure of proteins from UV circular dichroism spectra using an unsupervised learning neural network. Protein Eng 6:383–390

Bollen YJ, Nabuurs SM, van Berkel WJ, van Mierlo CP (2005) Last in, first out: the role of cofactor binding in flavodoxin folding. J Biol Chem 280:7836–7844

Cai K, Schirch D, Schirch V (1995) The affinity of pyridoxal 5′-phosphate for folding intermediates of *Escherichia coli* serine hydroxymethyltransferase. J Biol Chem 270:19294–19299

Choi YS, Han SK, Kim J, Yang JS, Jeon J, Ryu SH, Kim S (2010) ConPlex: a server for the evolutionary conservation analysis of protein complex structures. Nucleic Acids Res 38:W450–W456

Deu E, Kirsch JF (2007a) Cofactor-directed reversible denaturation pathways: the cofactor-stabilized Escherichia coli aspartate aminotransferase homodimer unfolds through a pathway that differs from that of the apoenzyme. Biochemistry 46:5819–5829

Deu E, Kirsch JF (2007b) The unfolding pathway for Apo *Escherichia coli* aspartate aminotransferase is dependent on the choice of denaturant. Biochemistry 46:5810–5818

Deu E, Dhoot J, Kirsch JF (2009) The partially folded homodimeric intermediate of Escherichia coli aspartate aminotransferase contains a "molten interface" structure. Biochemistry 48:433–441

Greene RF Jr, Pace CN (1974) Urea and guanidine hydrochloride denaturation of ribonuclease, lysozyme, alpha-chymotrypsin, and beta-lactoglobulin. J Biol Chem 249:5388–5393

Herold M, Leistler B, Hage A, Luger K, Kirschner K (1991) Autonomous folding and coenzyme binding of the excised pyridoxal 5′-phosphate binding domain of aspartate aminotransferase from *Escherichia coli*. Biochemistry 30:3612–3620

Hester G, Stark W, Moser M, Kallen J, Markovic-Housley Z, Jansonius JN (1999) Crystal structure of phosphoserine aminotransferase from Escherichia coli at 2.3 A resolution: comparison of the unligated enzyme and a complex with alpha-methyl-l-glutamate. J Mol Biol 286:829–850

Jansonius JN (1998) Structure, evolution and action of vitamin B6-dependent enzymes. Curr Opin Struct Biol 8:759–769

Kapetaniou EG, Thanassoulas A, Dubnovitsky AP, Nounesis G, Papageorgiou AC (2006) Effect of pH on the structure and stability of *Bacillus circulans* ssp. alkalophilus phosphoserine aminotransferase: thermodynamic and crystallographic studies. Proteins 63:742–753

Knapp JA, Pace CN (1974) Guanidine hydrochloride and acid denaturation of horse, cow, and *Candida krusei* cytochromes c. Biochemistry 13:1289–1294

Lakowicz JR (2006) Principles of fluorescence spectroscopy, 3rd edn. Springer, New York

Makhatadze GI, Privalov PL (1992) Protein interactions with urea and guanidinium chloride. A calorimetric study. J Mol Biol 226:491–505

Mehta PK, Hale TI, Christen P (1993) Aminotransferases: demonstration of homology and division into evolutionary subgroups. Eur J Biochem 214:549–561

Mishra V, Ali V, Nozaki T, Bhakuni V (2010) Entamoeba histolytica Phosphoserine aminotransferase (EhPSAT): insights into the structure-function relationship. BMC Res Notes 3:52

Muralidhara BK, Wittung-Stafshede P (2005) FMN binding and unfolding of Desulfovibrio desulfuricans flavodoxin: "hidden" intermediates at low denaturant concentrations. Biochim Biophys Acta 1747:239–250

Nandi PK, Robinson DR (1984) Effects of urea and guanidine hydrochloride on peptide and nonpolar groups. Biochemistry 23:6661–6668

Pant K, Crane BR (2005) Structure of a loose dimer: an intermediate in nitric oxide synthase assembly. J Mol Biol 352:932–940

Pettersen EF, Goddard TD, Huang CC, Couch GS, Greenblatt DM, Meng EC, Ferrin TE (2004) UCSF Chimera—a visualization system for exploratory research and analysis. J Comput Chem 25:1605–1612

Satterthwait AC, Jencks WP (1974) The mechanism of the aminolysis of acetate esters. J Am Chem Soc 96:7018–7031

Schellman JA (2002) Fifty years of solvent denaturation. Biophys Chem 96:91–101

Schneider G, Kack H, Lindqvist Y (2000) The manifold of vitamin B6 dependent enzymes. Structure 8:R1–R6

Schwede T, Kopp J, Guex N, Peitsch MC (2003) SWISS-MODEL: an automated protein homology-modeling server. Nucleic Acids Res 31:3381–3385

Singh K, Bhakuni V (2008) Toxoplasma gondii ferredoxin-NADP + reductase: role of ionic interactions in stabilization of native conformation and structural cooperativity. Proteins 71:1879–1888

Wardell SE, Kwok SC, Sherman L, Hodges RS, Edwards DP (2005) Regulation of the amino-terminal transcription activation domain of progesterone receptor by a cofactor-induced protein folding mechanism. Mol Cell Biol 25:8792–8808

West SM, Price NC (1989) The unfolding and refolding of cytoplasmic aspartate aminotransferase from pig heart. Biochem J 261:189–196